

Original Article

Cite this article: Sunthakar S, Parra DA, George-Durrett K, Crum K, Chew JD, Christensen J, Raucci FJ Jr, Xu M, Slaughter JC, and Soslow JH (2019) Tissue characterisation and myocardial mechanics using cardiac MRI in children with hypertrophic cardiomyopathy. *Cardiology in the Young* **29**: 1459–1467. doi: [10.1017/S1047951119002397](https://doi.org/10.1017/S1047951119002397)

Received: 22 April 2019

Revised: 1 September 2019

Accepted: 8 September 2019

First published online: 26 November 2019

Keywords:

Paediatric cardiology; hypertrophic cardiomyopathy; cardiac MRI; T1 mapping; myocardial strain


Author for correspondence:

Jonathan H. Soslow, MD, MSCI, Assistant Professor, Pediatrics, Thomas P. Graham, Jr. Division of Pediatric Cardiology, Monroe Carell Jr. Children's Hospital at Vanderbilt, 2200 Children's Way, Suite 5230, Doctors' Office Tower, Nashville, TN 37232-9119, USA.

Phone: +1 615 322 7447; Fax: +1 615 322 2210; E-mail: jonathan.h.soslow@vumc.org

[†]Current address: Division of Pediatric Cardiology, Department of Pediatrics, University of Nebraska Medical Center, Omaha, NE, USA

Tissue characterisation and myocardial mechanics using cardiac MRI in children with hypertrophic cardiomyopathy

Sudeep Sunthakar¹, David A. Parra², Kristen George-Durrett², Kimberly Crum², Joshua D. Chew², Jason Christensen^{2,†}, Frank J. Raucci, Jr², Meng Xu³, James C. Slaughter³ and Jonathan H. Soslow² 

¹Department of Pediatrics, Vanderbilt University Medical Center, Nashville, TN, USA; ²Thomas P Graham Division of Pediatric Cardiology, Department of Pediatrics, Vanderbilt University Medical Center, Nashville, TN, USA and ³Department of Biostatistics, Vanderbilt University Medical Center, Nashville, TN, USA

Abstract

Introduction: Distinguishing between hypertrophic cardiomyopathy and other causes of left ventricular hypertrophy can be difficult in children. We hypothesised that cardiac MRI T1 mapping could improve diagnosis of paediatric hypertrophic cardiomyopathy and that measures of myocardial function would correlate with T1 times and extracellular volume fraction. **Methods:** Thirty patients with hypertrophic cardiomyopathy completed MRI with tissue tagging, T1-mapping, and late gadolinium enhancement. Left ventricular circumferential strain was calculated from tagged images. T1, partition coefficient, and synthetic extracellular volume were measured at base, mid, apex, and thickest area of myocardial hypertrophy. MRI measures compared to cohort of 19 healthy children and young adults. Mann–Whitney U, Spearman's rho, and multivariable logistic regression were used for statistical analysis. **Results:** Hypertrophic cardiomyopathy patients had increased left ventricular ejection fraction and indexed mass. Hypertrophic cardiomyopathy patients had decreased global strain and increased native T1 (−14.3% interquartile range [−16.0, −12.1] versus −17.3% [−19.0, −15.7], $p < 0.001$ and 1015 ms [991, 1026] versus 990 ms [972, 1001], $p = 0.019$). Partition coefficient and synthetic extracellular volume were not increased in hypertrophic cardiomyopathy. Global native T1 correlated inversely with ejection fraction ($\rho = -0.63$, $p = 0.002$) and directly with global strain ($\rho = 0.51$, $p = 0.019$). A logistic regression model using ejection fraction and native T1 distinguished between hypertrophic cardiomyopathy and control with an area under the receiver operating characteristic curve of 0.91. **Conclusion:** In this cohort of paediatric hypertrophic cardiomyopathy, strain was decreased and native T1 was increased compared with controls. Native T1 correlated with both ejection fraction and strain, and a model using native T1 and ejection fraction differentiated patients with and without hypertrophic cardiomyopathy.

Hypertrophic cardiomyopathy is the leading cause of sudden cardiac death in healthy young athletes.¹ Hallmarks of the disease include ventricular hypertrophy, myocyte disarray, and both replacement and interstitial fibrosis. Distinguishing between hypertrophic cardiomyopathy and other causes of left ventricular hypertrophy can be difficult. Cardiac MRI has significant advantages over echocardiography for assessment of adults with hypertrophic cardiomyopathy, and newer methods of tissue characterisation may aid in the diagnosis of children with hypertrophic cardiomyopathy.²

The longitudinal relaxation time constant, or T1, can be measured non-invasively in myocardium using cardiac MRI. Native T1 maps, or maps obtained prior to contrast administration, can be analysed separately or combined with post-contrast T1 maps to derive either a partition coefficient or an extracellular volume fraction. Native T1 and extracellular volume are surrogates of extracellular matrix expansion³ and have been validated histologically.^{4–7}

Studies demonstrate lower myocardial strain in areas of replacement fibrosis in paediatric hypertrophic cardiomyopathy.⁸ Interstitial fibrosis also seems to have an effect on myocardial mechanics in multiple cardiovascular disease states, but this has never been studied in paediatric hypertrophic cardiomyopathy.^{9–11} A better understanding of the underlying relationship between myocardial mechanics and markers of fibrosis and myocyte hypertrophy may help clarify disease progression and inform future treatment strategies. The objectives of this study were to evaluate whether T1 mapping, partition coefficient, and extracellular volume mapping improve accuracy of diagnosis in patients with hypertrophic cardiomyopathy and to define the relationship between T1 and extracellular volume mapping and measures of myocardial function, particularly myocardial strain and left ventricular ejection fraction.

Methods

Enrollment

The Vanderbilt Institutional Review Board approved this retrospective study, and the study was performed in accordance with the ethical standards as laid down in the 1964 Declaration of Helsinki and its later amendments or comparable ethical standards. Patients who underwent cardiac MRI between 2015 and 2018 were identified from the paediatric cardiac MRI database. Inclusion criteria were children with a diagnosis of hypertrophic cardiomyopathy and prior cardiac MRI that included a modified Look-Locker inversion recovery. All hypertrophic cardiomyopathy patients had a definitive diagnosis based on family history and either a positive genotype or a phenotype consistent with hypertrophic cardiomyopathy ($n = 11$), clinical diagnosis with pathologic hypertrophy and known hypertrophic cardiomyopathy causing mutation, or definitive clinical diagnosis of hypertrophic cardiomyopathy with negative genetic testing ($n = 14$). Patients were excluded if they had an underlying neurologic, metabolic, or other secondary cause of hypertrophic cardiomyopathy, inadequate modified Look-Locker inversion recovery image quality for analysis. Genotype positive phenotype negative was defined as a patient with a known positive genotype but with clinical testing that would not meet criteria for definitive diagnosis of hypertrophic cardiomyopathy.

Control images for our study were acquired from 19 patients, 12–30 years of age, from previous cohorts of either clinically indicated cardiac MRIs or research cardiac MRIs. All controls had normal cardiac MRIs. Exclusion criteria for control cohort were cardiovascular disease, risk factors for cardiovascular disease, muscular dystrophy or unexplained skeletal muscle weakness, any diagnosis that could affect cardiac function or lead to myocardial fibrosis, and contraindication to cardiac MRI with gadolinium. All patients undergoing research cardiac MRI were aged 18–30 and previously healthy. For patients undergoing clinically indicated cardiac MRIs, indications were concern for possible arrhythmogenic right ventricular cardiomyopathy due to either an abnormal electrocardiogram or history of premature ventricular contractions with normal work-up, including normal cardiac MRI, and arrhythmogenic right ventricular cardiomyopathy ruled out; concern for abnormal left ventricular function on echocardiogram with normal function on cardiac MRI; evaluation for possible apical hypertrophic cardiomyopathy with normal cardiac MRI; and evaluation of atypical chest pain with normal work-up.

The electronic medical record was reviewed for genetic test results, Holter monitor results, treatment interventions (pharmacologic management, placement of implantable cardioverter defibrillator or pacemaker, or septal myectomy), and risk stratification criteria for hypertrophic cardiomyopathy (septal thickness greater than 30 mm, history of ventricular tachycardia or unexplained syncope, family history of hypertrophic cardiomyopathy with sudden cardiac death or aborted sudden cardiac death, and inadequate blood pressure response during treadmill test).

Cardiac MRI acquisition

Cardiac MRI was performed on a 1.5 Tesla Siemens Avanto. Functional imaging was performed as previously described using balanced steady-state free precession images in a short-axis stack.¹² Intravenous gadolinium contrast (gadopentate dimeglumine, Magnevist®, Bayer Healthcare Pharmaceuticals, Wayne, NJ, USA or gadobutrol, Gadovist®, Bayer Healthcare Pharmaceuticals,

Wayne, NJ, USA) was administered through a peripheral intravenous line at a dose of 0.2 mmol/kg. Late gadolinium enhancement imaging was performed using single shot (balanced steady-state free precession) and segmented (turboflash) inversion recovery with optimised inversion recovery to null the signal from the myocardium, as well as phase-sensitive inversion recovery balanced steady-state free precession with an inversion time of 300 ms.

Myocardial tagging was performed in the short axis at the base, level of the papillary muscles, and apex using a segmented k-space fast gradient echo sequence with electrocardiogram triggering. Grid tagging was performed with a spacing of 8 mm and 9–13 phases. Typical imaging parameters included slice thickness 6–8 mm, field of view $340 \times 340 \text{ mm}^2$, matrix size 256×192 , and minimum echo time and repetition time. The sequences were breath-holds and parallel imaging with generalised autocalibrating partially parallel acquisition with an acceleration factor of 2 was used. One patient had individual horizontal and vertical tagging performed, and in one patient, tagged images were not analysable.

Breath-held modified Look-Locker inversion recovery sequences were performed prior to and 15 minutes after contrast administration at the left ventricular base, mid-left ventricle, and apex in the short-axis plane.¹³ Modified Look-Locker inversion recovery sequences were motion-corrected, electrocardiogram-triggered images obtained in diastole with typical imaging parameters: non-selective inversion with a 35° flip angle, single-shot steady-state free precession imaging, initial inversion time of 120 ms with 80 ms increments, field of view $340 \times 272 \text{ mm}^2$, matrix size 256×144 , slice thickness 8 mm, voxel size $1.3 \times 1.9 \times 8.0 \text{ mm}^3$, repetition time of 2.6 ms, echo time of 1.1 ms, parallel imaging factor of 2. The matrix size was decreased to 192×128 for heart rates >90 (approximate voxel size $1.8 \times 2.1 \times 8 \text{ mm}^3$). The pre-contrast modified Look-Locker inversion recovery acquired five images after the first inversion with the equivalent of a 3 second pause followed by three images after the second inversion, or 5(3s)3 (as a true 3 second pause is not possible with the current software package, the number of heartbeats used for recovery was varied depending on the average heart rate measured just prior to T1 mapping, with 3 beats used for a heart rate of 60, 4 beats used for a heart rate of 80, 5 beats for a heart rate of 100, and 6 beats for a heart rate of 120; no patient had a heart rate over 120 in this study). The post-contrast protocol was acquired at a 4(1)3(1)2, or four images acquired after the first inversion with a 1 beat pause followed by a second inversion after which three images were acquired, an additional 1 beat pause, then a final inversion after which two images were acquired.¹⁴ Motion correction as described by Xue et al was performed, and a T1 map was generated on the scanner.¹⁵ A goodness-of-fit map was also performed at the time of the scan to evaluate data quality. In six hypertrophic cardiomyopathy patients, the modified Look-Locker inversion recovery was only performed at the mid-left ventricle slice; the basilar slice was deemed inadequate for analysis in one patient and the apical slice in two patients with hypertrophic cardiomyopathy.

Cardiac MRI post-processing

Left ventricular volume, mass, and function were calculated as previously described.¹⁶ The presence or absence of late gadolinium enhancement was qualitatively assessed. Percent of scar was calculated using the 5 standard deviation method on Medis (Medis Medical Imaging Systems, Leiden, The Netherlands) on the phase-sensitive inversion recovery images as per our labs standard protocol. Analysis of myocardial tagged images was performed as previously

described using harmonic phase methodology (Diagnosoft Inc., Morrisville, NC, USA).¹⁷ In brief, a contour or mesh was drawn over the tagged image at peak systole by outlining the epicardium and endocardium. The superior right ventricular insertion was identified manually. The contours were performed by the same reader (SS) with verification of each contour by a second reader (JHS) with more than 7 years of experience using the software. The software then calculated the global peak circumferential strain and the circumferential strain values for each segment (16 segment model) and slice (base, mid, and apex).

Using software programmed in MATLAB 2014a (The MathWorks, Natick, MA, USA), regions of interest were manually drawn on native and post-contrast T1 maps within the left ventricular mesocardium in 16 segments using the standard American Heart Association model of segmentation.¹⁸ These regions of interest were contoured by one reader with experience analysing T1 maps and confirmed by a second reader with 6 years of experience in analysing T1 mapping. To evaluate reproducibility, a second reader with experience analysing T1 maps repeated the analysis at the base, mid, and apex in a random sample of 10 hypertrophic cardiomyopathy patients on both the native and post-contrast maps. In addition, hypertrophic cardiomyopathy patients with significant left ventricular hypertrophy (left ventricular thickness >15 mm) had a region of interest drawn in the region of thickest hypertrophy. Only 10 hypertrophic cardiomyopathy patients had concurrent haematocrit levels, so extracellular volume maps were not analysed; instead, synthetic extracellular volume was calculated as described below. Regions of interest were carefully traced to avoid partial volume averaging with blood pool or epicardial fat. Based on the T1 mapping consensus statement, areas of late gadolinium enhancement were not excluded as these areas were felt to be the most focal areas in a continuum of diffuse extracellular matrix expansion.¹⁹

Partition coefficient was calculated from the native and post-contrast T1 using the following equation:

$$\text{Partition coefficient} = \frac{\left(\frac{1}{\text{myocardial T1}_{\text{post}}}\right) - \left(\frac{1}{\text{myocardial T1}_{\text{pre}}}\right)}{\left(\frac{1}{\text{blood pool T1}_{\text{post}}}\right) - \left(\frac{1}{\text{blood pool T1}_{\text{pre}}}\right)}$$

Synthetic haematocrit was calculated from the following equation optimised to this magnet:²⁰

$$\text{Synthetic hematocrit} = \left(315.1 \cdot \left[\frac{1}{\text{T1 blood}}\right]\right) + 0.213$$

The basal, mid, and apical synthetic extracellular volume fraction was calculated from the native and post-contrast T1 and the synthetic haematocrit using the following equation:

$$\text{Synthetic extracellular volume} = \left[\frac{\left(\frac{1}{\text{myocardial T1}_{\text{post}}}\right) - \left(\frac{1}{\text{myocardial T1}_{\text{pre}}}\right)}{\left(\frac{1}{\text{blood pool T1}_{\text{post}}}\right) - \left(\frac{1}{\text{blood pool T1}_{\text{pre}}}\right)}\right] * (1 - \text{synthetic hematocrit})$$

In patients with adequate maps at all three slices, global myocardial T1, global partition coefficient, and global synthetic extracellular volume were calculated. Imaging artifact was not contoured. Segments were not included in the analysis if the bounds of the myocardium could not be distinguished from surrounding

tissue and blood pool or if image registration was inadequate in those segments.

Statistical analysis

Categorical variables were compared using a Chi-square or Fisher's exact test and continuous variables were compared using a Wilcoxon rank-sum test. Correlations between continuous variables were obtained using a Spearman's rho. Reproducibility of native and post-contrast T1 mapping was assessed using intraclass correlation coefficient for absolute agreement. We fit univariate logistic regression models to estimate the probability of hypertrophic cardiomyopathy evaluating the following pre-specified predictors: left ventricular ejection fraction, indexed left ventricular mass, percent late gadolinium enhancement, circumferential strain at mid-left ventricle, native T1 at mid-left ventricle, partition coefficient at mid-left ventricle, and synthetic extracellular volume at mid-left ventricle. The mid-left ventricle slice was used for circumferential strain and T1 mapping because some patients did not have adequate image quality to calculate these measures at either the apex or the base (and thus inadequate images to calculate global values). Multivariable analysis was then performed using those predictors that were significant to determine the best predictors of hypertrophic cardiomyopathy (a total of six models evaluated). Analyses were performed with IBM SPSS statistics, version 25.0 (Armonk, NY, USA: IBM Corp.). Study data were collected and managed using Research Electronic Data Capture tools hosted at Vanderbilt.²¹

Results

Demographics

Thirty hypertrophic cardiomyopathy patients met inclusion and exclusion criteria. The mean age of hypertrophic cardiomyopathy diagnosis was 14.0 ± 2.9 years and the mean age at cardiac MRI was 15.8 ± 2.2 . Nineteen hypertrophic cardiomyopathy patients (63%) were male, while 17 controls (89%) were male. Further demographics can be found in Table 1.

Genetic testing was completed in 28 patients, with 16 testing positive for known hypertrophic cardiomyopathy mutations (Table 2), 10 with negative testing, and 2 with variants of unknown significance. Six patients had an implantable cardioverter defibrillator placed and three had a history of implantable cardioverter defibrillator shock. One patient who did not meet criteria for implantable cardioverter defibrillator placement died during sleep. Thirteen patients had received pharmacotherapy at some point during their medical course, with beta-blockade the most common therapy. Risk factors for sudden cardiac death are listed in Table 2.

Standard cardiac measures

Hypertrophic cardiomyopathy patients had increased indexed left ventricular mass (median 79 g/m^2 interquartile range [65, 91] versus 57 g/m^2 [54, 62], $p < 0.001$) and increased left ventricular ejection fraction (69% [63, 71] versus 60% [58, 64], $p = 0.001$) in comparison to controls. The right ventricular ejection fraction was also higher in hypertrophic cardiomyopathy (64% [60, 68] versus 57% [55, 60], $p < 0.001$). The median maximal wall thickness of the left ventricle in the hypertrophic cardiomyopathy group was 18 mm [16, 22.5]. A total of 18 hypertrophic cardiomyopathy patients (65%) had late gadolinium enhancement, almost exclusively in areas of pathologic hypertrophy, though some patients

Table 1. Demographics

	Control n = 19	Hypertrophic cardiomyopathy n = 30
Age at cardiac MRI (years)	21.2 ± 5.3 (range 12–30)	15.8 ± 2.2 (range 10–19)
Male gender	17 (89%)	19 (63%)
Height (cm)	176 ± 13	170 ± 11
Weight (kg)	71 ± 12	85 ± 28
Body surface area (m ²)	1.9 ± 0.2	2.0 ± 0.4
Race		
Caucasian	11 (58%)	21 (70%)
African American	3 (16%)	3 (10%)
Asian	1 (5%)	1 (3%)
Other	0	2 (7%)
Mixed	1 (5%)	0
Unknown/unwilling to report	3 (16%)	3 (10%)
Hispanic/Latino	1 (5%)	4 (13%)

Data presented as mean ± standard deviation or n (percent).

Table 2. Clinical characteristics of hypertrophic cardiomyopathy patients

	n = 30
Age at diagnosis (years)	14.0 ± 2.9
Alive	29 (97%)
Genetic testing	28 (93%)
Positive for known genetic mutation	16 (57%)
Implantable cardioverter defibrillator placed	6 (20%)
Patients with implantable cardioverter defibrillator shocks delivered	3 (50%)
History of septal myectomy	3 (10%)
Use of medications	16 (53%)
Angiotensin converting enzyme inhibitor	1 (3%)
Beta-blocker	15 (50%)
Calcium channel blocker	1 (3%)
Aspirin	1 (3%)
Other	2 (10%)
Risk factors for sudden cardiac death	
Maximal septal thickness > 30 mm	3 (10%)
Syncope	6 (20%)
Family history of sudden cardiac death	11 (37%)
History of ventricular tachycardia	3 (10%)*
Inadequate blood pressure response to exercise	8 (27%)
History of aborted sudden death	2 (7%)

*All non-sustained ventricular tachycardia

had mild late gadolinium enhancement at the right ventricular insertion points. Patients with late gadolinium enhancement had a median percent scar of 3.3% [1.7, 5.1].

Myocardial strain and T1 mapping

The native and post-contrast T1 maps had good reproducibility (native T1: base intraclass correlation coefficient 0.89 $p = 0.001$, mid intraclass correlation coefficient 0.91 $p < 0.001$, apex intraclass correlation coefficient 0.90 $p = 0.001$; post-contrast T1: base intraclass correlation coefficient 0.95 $p < 0.001$, mid intraclass correlation coefficient 0.96 $p < 0.001$, apex intraclass correlation coefficient 0.94 $p < 0.001$). Hypertrophic cardiomyopathy patients had decreased global circumferential strain compared with controls as well as decreased circumferential strain at the base, mid-left ventricle, and apex (Table 3). For example, T1 maps and tagged images are demonstrated in Figure 1. Hypertrophic cardiomyopathy patients had significantly increased global and mid-native T1 compared with controls (Table 3 for all results, including basal and apical). The global and mid partition coefficient and synthetic extracellular volume were not significantly different between hypertrophic cardiomyopathy and control.

Native T1 in the area of maximal myocardial hypertrophy was increased compared to the median mid-left ventricle T1 of the control population (1027 ms [1004, 1047] versus 990 [964, 1004], $p = 0.001$). The partition coefficient and synthetic extracellular volume in the region of maximal hypertrophy were not statistically different between hypertrophic cardiomyopathy and control, suggesting the primary pathology in these regions may be due to myocyte hypertrophy and not extracellular matrix expansion.

Within the hypertrophic cardiomyopathy group, patients with late gadolinium enhancement had significantly increased mid-native T1 compared to those without late gadolinium enhancement; global native T1 was higher but did not reach statistical significance (Table 4 for all results, including basal and apical). The global and mid synthetic extracellular volume were also increased in hypertrophic cardiomyopathy patients with late gadolinium enhancement as were the global and mid partition coefficients (Table 4).

Within the hypertrophic cardiomyopathy group, left ventricular ejection fraction had a weak inverse correlation with percent late gadolinium enhancement ($\rho = -0.39$, $p = 0.035$) and a strong inverse correlation with global native T1 ($\rho = -0.63$, $p = 0.002$). Maximal wall thickness correlated with percent late gadolinium enhancement ($\rho = 0.63$, $p < 0.001$). Global T1 correlated with percent late gadolinium enhancement ($\rho = 0.44$, $p = 0.041$). Global circumferential strain correlated with global T1 ($\rho = 0.51$, $p = 0.019$) and indexed mass ($\rho = 0.63$, $p = 0.004$) but not with percent late gadolinium enhancement; however, a sub analysis comparing all segments with and without strain demonstrated worse strain in segments with late gadolinium enhancement (-11.1% [-8.1 , -14.2] versus -14.9 [-11.0 , -17.8], $p < 0.001$).

Global synthetic extracellular volume and partition coefficient did not correlate with left ventricular ejection fraction ($\rho = -0.3$, $p = 0.211$ and $\rho = -0.19$, $p = 0.432$) or global circumferential strain ($\rho = 0.09$, $p = 0.723$ and $\rho = 0.069$, $p = 0.785$). Both global synthetic extracellular volume and partition coefficient correlated with percent late gadolinium enhancement ($\rho = 0.51$, $p = 0.03$ and $\rho = 0.48$, $p = 0.039$).

Modelling

Univariate logistic regression analysis demonstrated that left ventricular ejection fraction, circumferential strain at the mid-left ventricle, native T1 at the mid-left ventricle, and indexed

Table 3. Comparison of cardiovascular MRI in control and hypertrophic cardiomyopathy patients

	Control		Hypertrophic cardiomyopathy		p-value
	n	Median (IQR)	n	Median (IQR)	
Left ventricular ejection fraction (%)	19	60 (58, 64)	30	69 (63, 71)	0.001
Left ventricular mass index (g/m ²)	19	57 (54, 62)	30	79 (65, 91)	<0.001
Right ventricular ejection fraction (%)	12	57 (55, 60)	30	64 (60, 68)	<0.001
Base circumferential strain (%)	19	-16.9 (-18.4, -16.7)	29	-14.0 (-15.7, -12.8)	<0.001
Mid circumferential strain (%)	19	-16.8 (-19.5, -15.2)	29	-14.3 (-16.0, -12.5)	0.001
Apex circumferential strain (%)	19	-18.4 (-20.5, -15.9)	28	-14.7 (-17.4, -10.7)	0.001
Global circumferential strain (%)	18	-17.3 (-19.9, -15.7)	28	-14.3 (-16.0, -12.1)	<0.001
Base T1 (ms)	19	996 (981, 1007)	23	1026 (989, 1039)	0.013
Mid T1 (ms)	19	990 (964, 1004)	30	1013 (986, 1036)	0.007
Apex T1 (ms)	18	983 (968, 1005)	23	996 (969, 1032)	0.237
Global T1 (ms)	18	990 (972, 1001)	22	1015 (991, 1026)	0.019
Base partition coefficient	19	0.39 (0.36, 0.39)	23	0.39 (0.35, 0.45)	0.850
Mid partition coefficient	19	0.39 (0.36, 0.43)	28	0.39 (0.37, 0.43)	0.948
Apex partition coefficient	17	0.42 (0.40, 0.45)	21	0.41 (0.37, 0.45)	0.437
Global partition coefficient	17	0.40 (0.39, 0.42)	19	0.39 (0.37, 0.46)	0.812
Base synthetic extracellular volume	19	0.23 (0.21, 0.23)	23	0.22 (0.20, 0.26)	0.950
Mid synthetic extracellular volume	19	0.23 (0.21, 0.25)	28	0.23 (0.21, 0.25)	0.931
Apex synthetic extracellular volume	17	0.25 (0.23, 0.26)	21	0.24 (0.21, 0.27)	0.271
Global synthetic extracellular volume	17	0.23 (0.22, 0.25)	19	0.23 (0.21, 0.27)	0.763

left ventricular mass were statistically significant in predicting presence of hypertrophic cardiomyopathy ($p < 0.05$ for all) (Table 5). Percent late gadolinium enhancement, partition coefficient at the mid-left ventricle, and synthetic extracellular volume at the mid-left ventricle were not significant in predicting hypertrophic cardiomyopathy. Six models were evaluated based on univariate regression results and the model with the highest receiver operating characteristic for prediction of hypertrophic cardiomyopathy included left ventricular ejection fraction and native T1 at the mid-left ventricle ($p = 0.001$ for left ventricular ejection fraction and $p = 0.003$ for native T1 at mid-left ventricle); this model had an area under the receiver operating characteristic curve of 0.91 (Fig 2a). However, a scatterplot displaying the predicted probabilities for this model demonstrated some overlap between patients with and without hypertrophic cardiomyopathy (Fig 2b).

Discussion

The primary findings of this study are that hypertrophic cardiomyopathy patients have increased native T1 compared with controls, native T1 correlates strongly with global circumferential strain and left ventricular ejection fraction, and modeling using multiple cardiac imaging markers may aid in diagnosis of hypertrophic cardiomyopathy.

While native T1 mapping correlated strongly with circumferential strain and left ventricular ejection fraction, the partition coefficient and synthetic extracellular volume did not. Even in the

thickest areas of pathologic hypertrophy, partition coefficient and synthetic extracellular volume were not significantly increased compared with controls. These findings may reflect an overall mild phenotype in this cohort, which would also be supported by the relatively low percent late gadolinium enhancement. As expected, the native T1, partition coefficient, and synthetic extracellular volume were increased in hypertrophic cardiomyopathy patients with late gadolinium enhancement. However, native T1 mapping detects abnormalities of both the extracellular matrix and the myocytes, while partition coefficient and synthetic extracellular volume are more specific for extracellular matrix expansion.²² We hypothesise that the increased native T1 times are primarily reflecting underlying structural abnormalities in the myocytes, not the extracellular matrix. Indeed, a study by Swaboda et al used multivariable modelling in adult hypertrophic cardiomyopathy patients to demonstrate a correlation between native T1 and myocardial mechanics but not extracellular volume fraction, suggesting that the structural abnormalities resulting in impaired function were cellular.²²

Previous studies in adult hypertrophic cardiomyopathy have demonstrated a statistically significant difference in native T1 between hypertrophic cardiomyopathy and controls.²³ Indeed, some reports have suggested that native T1 can be used to distinguish between patients with and without hypertrophic cardiomyopathy.^{24,25} The only paediatric study of which we are aware also demonstrated a significant difference between hypertrophic cardiomyopathy and controls.²⁶ While use of native T1 in isolation predicts a diagnosis of hypertrophic cardiomyopathy, there was significant overlap between groups. A model combining native

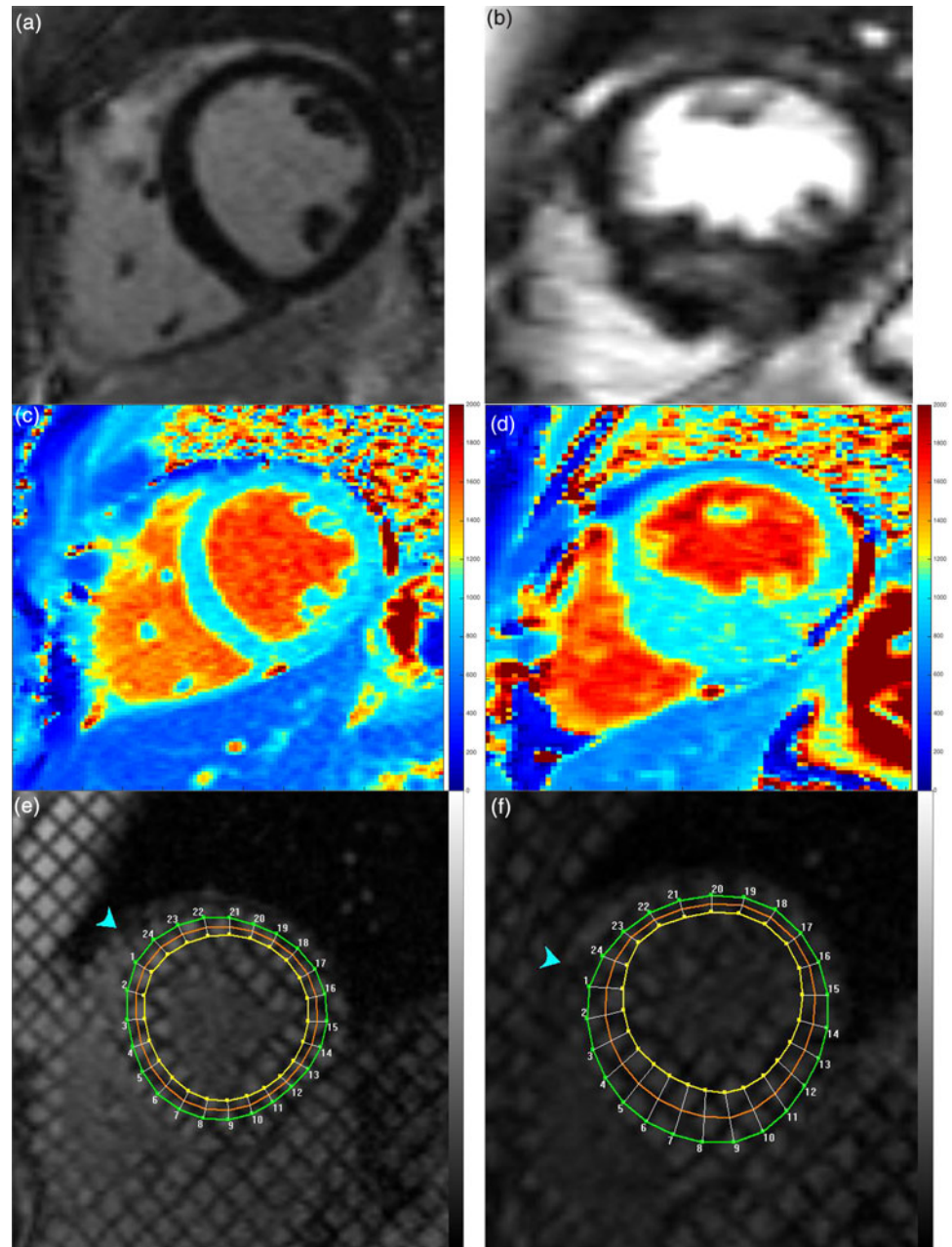


Figure 1. Example in healthy control (left column) and patient with hypertrophic cardiomyopathy (right column). (a) and (b) late gadolinium enhancement images, (c) and (d) native T1 maps, and (e) and (f) tagged images

T1 with left ventricular ejection fraction provided the highest area under the curve for diagnosis of hypertrophic cardiomyopathy. It is possible that a more comprehensive model that also includes circumferential strain and indexed left ventricular mass would improve segregation of groups, though we were unable to adequately evaluate a more comprehensive model due to sample size limitations.

Partial volume averaging, particularly at the apex or base, can lead to inaccuracies in T1 maps.²⁷ While we repeated and/or eliminated poor-quality maps, these data could skew the results at these slices. Of note, the model only included T1 mapping at the mid-left ventricle, so is much less likely to be affected by partial volume averaging.

Our patient cohort only included four patients who were genotype positive and phenotype negative, and it is unclear whether

this model can distinguish between patients with milder forms of hypertrophic cardiomyopathy and other causes of left ventricular hypertrophy. Evaluation of model performance in patients without late gadolinium enhancement demonstrated relatively good separation between hypertrophic cardiomyopathy and control (Fig 2c), but future studies should be performed comparing mild hypertrophic cardiomyopathy to patients with other causes of left ventricular hypertrophy. While this model is promising, the small sample size necessitates validation in a larger cohort of patients before using clinically. Our intent is to use this model as pilot data for future analyses of larger cohorts of patients with hypertrophic cardiomyopathy. We caution the use of this model in clinical practice at this time.

Left ventricular ejection fraction, indexed left ventricular mass, native T1, and circumferential strain are of particular interest for

Table 4. Comparison of native T1 mapping, partition coefficient, and synthetic extracellular volume in patients with hypertrophic cardiomyopathy with and without late gadolinium enhancement

	Hypertrophic cardiomyopathy with late gadolinium enhancement		Hypertrophic cardiomyopathy without late gadolinium enhancement		p-value
	n	Median (IQR)	n	Median (IQR)	
Base T1 (ms)	14	1032 (1006, 1042)	9	1002 (971, 1029)	0.038
Mid T1 (ms)	18	1019 (1009, 1045)	12	986 (960, 1034)	0.034
Apex T1 (ms)	14	1006 (983, 1038)	9	969 (957, 1011)	0.044
Global T1 (ms)	13	1017 (1006, 1027)	9	990 (962, 1029)	0.10
Base partition coefficient	14	0.39 (0.37, 0.46)	9	0.36 (0.34, 0.38)	0.059
Mid partition coefficient	17	0.41 (0.38, 0.45)	11	0.37 (0.34, 0.39)	0.037
Apex partition coefficient	14	0.43 (0.40, 0.47)	7	0.37 (0.36, 0.39)	0.035
Global partition coefficient	12	0.42 (0.39, 0.46)	7	0.37 (0.34, 0.38)	0.023
Base synthetic extracellular volume	14	0.23 (0.21, 0.27)	9	0.21 (0.19, 0.22)	0.014
Mid synthetic extracellular volume	17	0.24 (0.22, 0.26)	11	0.21 (0.20, 0.22)	0.025
Apex synthetic extracellular volume	14	0.25 (0.23, 0.27)	7	0.21 (0.21, 0.23)	0.028
Global synthetic extracellular volume	12	0.25 (0.22, 0.27)	7	0.20 (0.20, 0.22)	0.038

Table 5. Univariate logistic regression modelling with diagnosis of hypertrophic cardiomyopathy as outcome

	Univariate analysis
Left ventricular ejection fraction	0.005
Indexed left ventricular mass	0.004
Percent late gadolinium enhancement	0.990
Circumferential strain at mid-left ventricle	0.003
Native T1 at mid-left ventricle	0.012
Partition coefficient at mid-left ventricle	0.952
Synthetic extracellular volume fraction at mid-left ventricle	0.927

Bold values reached our definition of statistical significance, as defined by $p < 0.05$.

hypertrophic cardiomyopathy diagnosis because all measures can be obtained without the use of contrast, allowing for shorter scan times and decreasing exposure to gadolinium. Moreover, these measures provide a combination of structural and functional measures for diagnosis. Further studies in a larger cohort could help clarify the diagnostic utility in patients with mild disease and allow for expansion of the number of predictors, potentially improving the model results. These studies should include patients with other causes of hypertrophy, such as hypertension or athlete's heart, to further evaluate whether native T1 can effectively distinguish between patients with and without hypertrophic cardiomyopathy.

Limitations

This study is limited by a small sample size. In addition, only a small number of patients had haematocrit values drawn at the same time as the cardiac MRIs, so calculation of the extracellular

volume was not possible. We elected to use a locally derived model to calculate synthetic extracellular volume. While our previous data suggested that synthetic extracellular volume can lead to clinical errors in individual patients, our data demonstrated that synthetic extracellular volume correlates well with extracellular volume and can be used in research cohorts such as this one.²⁰ Given the difficulty in obtaining paediatric control values, particularly for extracellular volume, our age and gender distribution did not match perfectly between hypertrophic cardiomyopathy and controls.²⁸ Per protocol, the modified Look-Locker inversion recovery sequences were performed in one slice at the base, mid-left ventricle, and apex. Because of this, it was possible that the thickest segment on the T1 maps did not perfectly correspond to the patient's thickest segment on cine imaging. Placement of modified Look-Locker inversion recovery sequences through the segments with largest pathological hypertrophy could increase the difference we detected between native T1 of the thickest segments and controls.

Some patients with hypertrophic cardiomyopathy did not have either basal ($n = 7$) or apical ($n = 8$) T1 mapping analysed as the maps were either not performed or were inadequate. These patients were included in the analysis for all available slices but the missing data could have skewed the results. The change in contrast agents, which have different relaxivity, may have affected late gadolinium enhancement or extracellular volume assessment but was unavoidable as the contrast change was made institution-wide. While some studies suggest that late gadolinium enhancement is more apparent with Gadovist than Magnevist, others suggest similar images for the two contrast agents.²⁹⁻³¹ Though there are minimal available data comparing extracellular volume values with Gadovist and Magnevist, the extracellular volume appears to be relatively contrast independent, with no significant difference or differences of questionable clinical significance between contrast agents.³²⁻³⁴

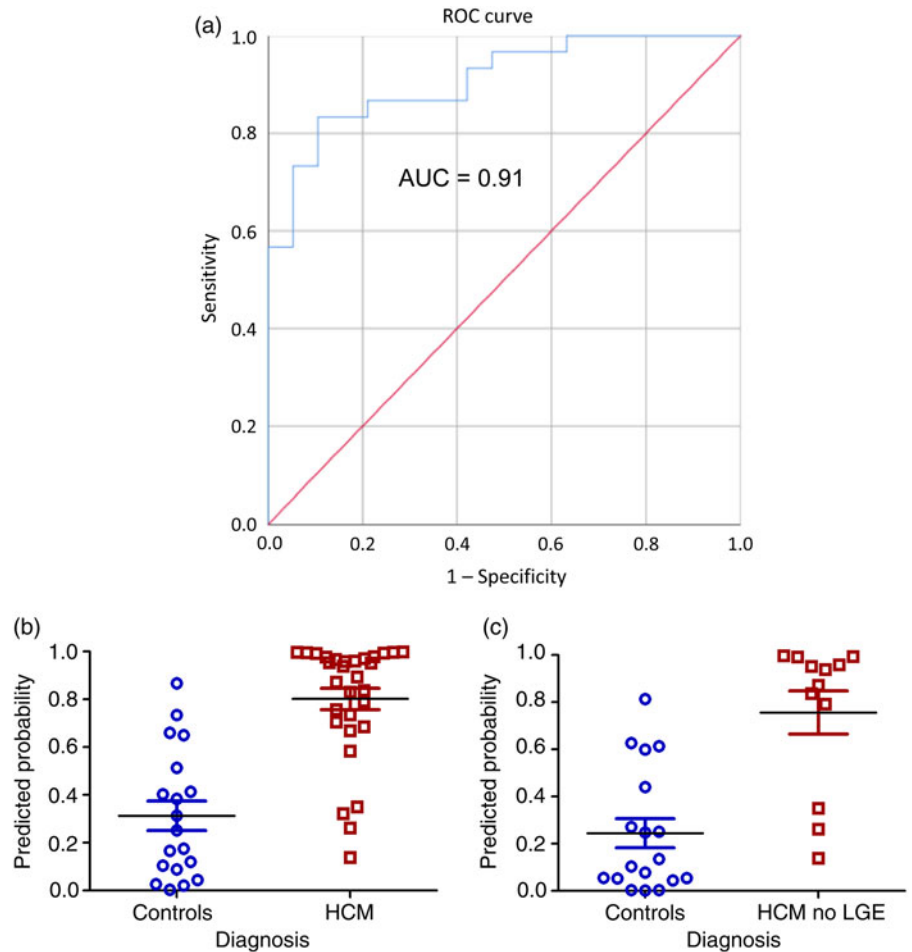


Figure 2. (a) Receiver operating characteristic curve for model using left ventricular ejection fraction and native T1 at the mid-left ventricle to predict a diagnosis of hypertrophic cardiomyopathy. (b) Scatterplot of model results demonstrates some overlap in patients with and without hypertrophic cardiomyopathy. (c) Scatterplot of same model only in patients without late gadolinium enhancement (milder disease) again demonstrates some overlap of patients with and without hypertrophic cardiomyopathy.

Conclusions

In this cohort of hypertrophic cardiomyopathy, native T1 was increased in hypertrophic cardiomyopathy compared with control. Native T1 also correlated with circumferential strain, suggesting a relationship between structural and functional abnormalities in paediatric hypertrophic cardiomyopathy. A model including left ventricular ejection fraction and native T1 may aid in the diagnosis of children with hypertrophic cardiomyopathy.

Acknowledgements. The authors would like to acknowledge the developers of the pulse sequence and reconstruction software: Bruce Spottiswoode, Andreas Greiser, Hui Xue, Christopher Glielmi, Shivraman Giri, and Randall Kroeker.

Author Contributions. SS, JHS, and DAP conceived and designed the study, acquired, analysed, and interpreted the data, and drafted the manuscript. KGD, KC, FJR, JC, and JDC helped with data collection and analysis and critically reviewed the manuscript. MX and JCS helped perform statistical analysis and critically reviewed the manuscript. All authors read and approved the final manuscript.

Financial Support. Research reported in this publication was supported by the National Heart, Lung, and Blood Institute of the National Institutes of Health under Award Number K23HL123938 (Bethesda, MD, USA) (Soslow). The content is solely the responsibility of the authors and does not necessarily represent the official views of the National Institutes of Health.

The project described was supported by CTSA award No. ULI TR002243 from the National Center for Advancing Translational Sciences. Its contents are solely the responsibility of the authors and do not necessarily represent official

views of the National Center for Advancing Translational Sciences or the National Institutes of Health.

This work was supported by Haley's Heart Foundation.

Conflicts of Interest. None.

Ethical Standards. The authors assert that all procedures contributing to this work comply with the ethical standards of the relevant national guidelines on human experimentation and with the Helsinki Declaration of 1975, as revised in 2008, and has been approved by the Vanderbilt Institutional Review Board.

References

1. Maron BJ, Doerer JJ, Haas TS, Tierney DM, Mueller FO. Sudden deaths in young competitive athletes: analysis of 1866 deaths in the United States, 1980-2006. *Circulation* 2009; 119: 1085-1092. doi: [10.1161/CIRCULATIONAHA.108.804617](https://doi.org/10.1161/CIRCULATIONAHA.108.804617)
2. Patel AR, Kramer CM. Role of cardiac magnetic resonance in the diagnosis and prognosis of nonischemic cardiomyopathy. *JACC Cardiovasc Imaging* 2017; 10 (10 Pt A): 1180-1193. doi: [10.1016/j.jcmg.2017.08.005](https://doi.org/10.1016/j.jcmg.2017.08.005)
3. Kellman P, Wilson JR, Xue H, Ugander M, Arai AE. Extracellular volume fraction mapping in the myocardium, part 1: evaluation of an automated method. *J Cardiovasc Magn Reson* 2012; 14: 63. doi: [10.1186/1532-429X-14-63](https://doi.org/10.1186/1532-429X-14-63)
4. Miller CA, Naish JH, Bishop P, et al. Comprehensive validation of cardiovascular magnetic resonance techniques for the assessment of myocardial extracellular volume. *Circ Cardiovasc Imaging* 2013; 6: 373-383. doi: [10.1161/CIRCIMAGING.112.000192](https://doi.org/10.1161/CIRCIMAGING.112.000192)
5. Flett AS, Hayward MP, Ashworth MT, et al. Equilibrium contrast cardiovascular magnetic resonance for the measurement of diffuse myocardial

- fibrosis: preliminary validation in humans. *Circulation* 2010; 122: 138–144. doi: [10.1161/CIRCULATIONAHA.109.930636](https://doi.org/10.1161/CIRCULATIONAHA.109.930636)
6. Iles LM, Ellims AH, Llewellyn H, et al. Histological validation of cardiac magnetic resonance analysis of regional and diffuse interstitial myocardial fibrosis. *Eur Heart J Cardiovasc Imaging* 2015; 16: 14–22. doi: [10.1093/ehjci/jeu182](https://doi.org/10.1093/ehjci/jeu182)
 7. Child N, Suna G, Dabir D, et al. Comparison of MOLLI, shMOLLI, and SASHA in discrimination between health and disease and relationship with histologically derived collagen volume fraction. *Eur Heart J Cardiovasc Imaging* 2018; 19(7): 768–776. doi: [10.1093/ehjci/jex309](https://doi.org/10.1093/ehjci/jex309)
 8. Bogarapu S, Puchalski MD, Everitt MD, Williams RV, Weng HY, Menon SC. Novel Cardiac Magnetic Resonance Feature Tracking (CMR-FT) analysis for detection of myocardial fibrosis in pediatric hypertrophic cardiomyopathy. *Pediatr Cardiol* 2016; 37: 663–673. doi: [10.1007/s00246-015-1329-8](https://doi.org/10.1007/s00246-015-1329-8)
 9. Wu LM, An DL, Yao QY, et al. Hypertrophic cardiomyopathy and left ventricular hypertrophy in hypertensive heart disease with mildly reduced or preserved ejection fraction: insight from altered mechanics and native T1 mapping. *Clin Radiol* 2017; 72: 835–843. doi: [10.1016/j.crad.2017.04.019](https://doi.org/10.1016/j.crad.2017.04.019)
 10. Haggerty CM, Suever JD, Pulenthiran A, et al. Association between left ventricular mechanics and diffuse myocardial fibrosis in patients with repaired Tetralogy of Fallot: a cross-sectional study. *J Cardiovasc Magn Reson* 2017; 19: 100. doi: [10.1186/s12968-017-0410-2](https://doi.org/10.1186/s12968-017-0410-2)
 11. Siegel B, Olivieri L, Gordish-Dressman H, Spurney CF. Myocardial strain using cardiac MR feature tracking and speckle tracking echocardiography in duchenne muscular dystrophy patients. *Pediatr Cardiol* 2018; 39(3): 478–483. doi: [10.1007/s00246-017-1777-4](https://doi.org/10.1007/s00246-017-1777-4). [Epub 2017 Nov 29].
 12. Schulz-Menger J, Bluemke DA, Bremerich J, et al. Standardized image interpretation and post processing in cardiovascular magnetic resonance: society for Cardiovascular Magnetic Resonance (SCMR) board of trustees task force on standardized post processing. *J Cardiovasc Magn Reson* 2013; 15: 35. doi: [10.1186/1532-429X-15-35](https://doi.org/10.1186/1532-429X-15-35)
 13. Messroghli DR, Radjenovic A, Kozierke S, Higgins DM, Sivananthan MU, Ridgway JP. Modified Look-Locker inversion recovery (MOLLI) for high-resolution T1 mapping of the heart. *Magn Reson Med* 2004; 52: 141–146. doi: [10.1002/mrm.20110](https://doi.org/10.1002/mrm.20110)
 14. Kellman P, Hansen MS. T1-mapping in the heart: accuracy and precision. *J Cardiovasc Magn Reson* 2014; 16: 2. doi: [10.1186/1532-429X-16-2](https://doi.org/10.1186/1532-429X-16-2)
 15. Xue H, Shah S, Greiser A, et al. Motion correction for myocardial T1 mapping using image registration with synthetic image estimation. *Magn Reson Med* 2012; 67: 1644–1655. doi: [10.1002/mrm.23153](https://doi.org/10.1002/mrm.23153)
 16. Soslow JH, Damon BM, Saville BR, et al. Evaluation of post-contrast myocardial t1 in duchenne muscular dystrophy using cardiac magnetic resonance imaging. *Pediatr Cardiol* 2015; 36: 49–56. doi: [10.1007/s00246-014-0963-x](https://doi.org/10.1007/s00246-014-0963-x)
 17. Simpson SA, Field SL, Xu M, Saville BR, Parra DA, Soslow JH. Effect of weight extremes on ventricular volumes and myocardial strain in repaired tetralogy of fallot as measured by CMR. *Pediatr Cardiol*. 2017. doi: [10.1007/s00246-017-1793-4](https://doi.org/10.1007/s00246-017-1793-4)
 18. Cerqueira MD, Weissman NJ, Dilsizian V, et al. Standardized myocardial segmentation and nomenclature for tomographic imaging of the heart. A statement for healthcare professionals from the cardiac imaging committee of the council on clinical cardiology of the american heart association. *Circulation* 2002; 105: 539–542.
 19. Moon JC, Messroghli DR, Kellman P, et al. Myocardial T1 mapping and extracellular volume quantification: a Society for Cardiovascular Magnetic Resonance (SCMR) and CMR working group of the european society of cardiology consensus statement. *J Cardiovasc Magn Reson* 2013; 15: 92. doi: [10.1186/1532-429X-15-92](https://doi.org/10.1186/1532-429X-15-92)
 20. Raucci FJ, Jr., Parra DA, Christensen JT, et al. Synthetic hematocrit derived from the longitudinal relaxation of blood can lead to clinically significant errors in measurement of extracellular volume fraction in pediatric and young adult patients. *J Cardiovasc Magn Reson* 2017; 19: 58. doi: [10.1186/s12968-017-0377-z](https://doi.org/10.1186/s12968-017-0377-z)
 21. Harris PA, Taylor R, Thielke R, Payne J, Gonzalez N, Conde JG. Research electronic data capture (REDCap)—a metadata-driven methodology and workflow process for providing translational research informatics support. *J Biomed Inform* 2009; 42: 377–381. doi: [10.1016/j.jbi.2008.08.010](https://doi.org/10.1016/j.jbi.2008.08.010)
 22. Swoboda PP, McDiarmid AK, Erhayiem B, et al. Effect of cellular and extracellular pathology assessed by T1 mapping on regional contractile function in hypertrophic cardiomyopathy. *J Cardiovasc Magn Reson* 2017; 19: 16. doi: [10.1186/s12968-017-0334-x](https://doi.org/10.1186/s12968-017-0334-x)
 23. van den Boomen M, Slart R, Hulleman EV, et al. Native T1 reference values for nonischemic cardiomyopathies and populations with increased cardiovascular risk: a systematic review and meta-analysis. *J Magn Reson Imaging* 2018; 47: 891–912. doi: [10.1002/jmri.25885](https://doi.org/10.1002/jmri.25885)
 24. Hinojar R, Varma N, Child N, et al. T1 mapping in discrimination of hypertrophic phenotypes: hypertensive heart disease and hypertrophic cardiomyopathy: findings from the international T1 multicenter cardiovascular magnetic resonance study. *Circ Cardiovasc Imaging* 2015; 8(12): pii: e003285. doi: [10.1161/CIRCIMAGING.115.003285](https://doi.org/10.1161/CIRCIMAGING.115.003285)
 25. Puntmann VO, Voigt T, Chen Z, et al. Native T1 mapping in differentiation of normal myocardium from diffuse disease in hypertrophic and dilated cardiomyopathy. *JACC Cardiovasc Imaging* 2013; 6: 475–484. doi: [10.1016/j.jcmg.2012.08.019](https://doi.org/10.1016/j.jcmg.2012.08.019)
 26. Parekh K, Markl M, Deng J, de Freitas RA, Rigsby CK. T1 mapping in children and young adults with hypertrophic cardiomyopathy. *Int J Cardiovasc Imaging* 2017; 33: 109–117. doi: [10.1007/s10554-016-0979-9](https://doi.org/10.1007/s10554-016-0979-9)
 27. Messroghli DR, Moon JC, Ferreira VM, et al. Clinical recommendations for cardiovascular magnetic resonance mapping of T1, T2, T2* and extracellular volume: a consensus statement by the Society for Cardiovascular Magnetic Resonance (SCMR) endorsed by the European Association for Cardiovascular Imaging (EACVI). *J Cardiovasc Magn Reson* 2017; 19: 75. doi: [10.1186/s12968-017-0389-8](https://doi.org/10.1186/s12968-017-0389-8)
 28. Rosmini S, Bulluck H, Captur G, et al. Myocardial native T1 and extracellular volume with healthy ageing and gender. *Eur Heart J Cardiovasc Imaging* 2018; 19: 615–621. doi: [10.1093/ehjci/jeu034](https://doi.org/10.1093/ehjci/jeu034)
 29. De Cobelli F, Esposito A, Perseghin G, et al. Intraindividual comparison of gadobutrol and gadopentetate dimeglumine for detection of myocardial late enhancement in cardiac MRI. *AJR Am J Roentgenol* 2012; 198: 809–816. doi: [10.2214/AJR.11.7118](https://doi.org/10.2214/AJR.11.7118)
 30. Rudolph A, Messroghli D, von Knobelsdorff-Brenkenhoff F, et al. Prospective, randomized comparison of gadopentetate and gadobutrol to assess chronic myocardial infarction applying cardiovascular magnetic resonance. *BMC Med Imaging* 2015; 15: 55. doi: [10.1186/s12880-015-0099-3](https://doi.org/10.1186/s12880-015-0099-3)
 31. Liu D, Ma X, Liu J, et al. Quantitative analysis of late gadolinium enhancement in hypertrophic cardiomyopathy: comparison of diagnostic performance in myocardial fibrosis between gadobutrol and gadopentetate dimeglumine. *Int J Cardiovasc Imaging* 2017; 33: 1191–1200. doi: [10.1007/s10554-017-1101-7](https://doi.org/10.1007/s10554-017-1101-7)
 32. Kawel N, Nacif M, Zavodni A, et al. T1 mapping of the myocardium: intra-individual assessment of post-contrast T1 time evolution and extracellular volume fraction at 3T for Gd-DTPA and Gd-BOPTA. *J Cardiovasc Magn Reson* 2012; 14: 26. doi: [10.1186/1532-429X-14-26](https://doi.org/10.1186/1532-429X-14-26)
 33. Rahsepar AA, Ghasemiesfe A, Suwa K, et al. Comprehensive evaluation of macroscopic and microscopic myocardial fibrosis by cardiac MR: intra-individual comparison of gadobutrol versus gadoterate meglumine. *Eur Radiol*. 2019. doi: [10.1007/s00330-018-5956-3](https://doi.org/10.1007/s00330-018-5956-3)
 34. Kawel N, Nacif M, Zavodni A, et al. T1 mapping of the myocardium: intra-individual assessment of the effect of field strength, cardiac cycle and variation by myocardial region. *J Cardiovasc Magn Reson* 2012; 14: 27. doi: [10.1186/1532-429X-14-27](https://doi.org/10.1186/1532-429X-14-27)